Modeling of Diffusion and Concurrent Metabolism in Cutaneous Tissue

Peter Boderke[*], Klaus Schittkowski[§], Manfred Wolf[#] and Hans P. Merkle[*]

[*]Department of Pharmacy, Swiss Federal Institute of Technology Zurich (ETH), Zürich, Switzerland

[§]Department of Mathematics, University of Bayreuth, Bayreuth, Germany

[#]Department of Pharmacy, Pharmaceutical Technology, University of Bonn, Bonn, Germany

running head: Diffusion and metabolism in metabolically active tissue

Corresponding Author: Prof. Hans P. Merkle, Swiss Federal Institute of Technology Zurich (ETH), Winterthurerstr. 190, CH-8057 Zürich, Switzerland

phone: 41-1-635-6011, fax: 41-1-635 6881

e-mail: hmerkle@pharma.ethz.ch

Abstract

A physical model is described, which considers diffusion and simultaneous saturable Michaelis-Menten metabolism of a drug within the metabolizing layer of the skin. The program EASY-FIT was used to numerically generate substrate concentration profiles within the tissue and resulting substrate fluxes out of the tissue for various parameters, i.e. diffusion coefficient D, substrate partition coefficient P, tissue thickness L and maximum metabolic rate V_{max} in order to describe their effect on the kinetics of drug permeation. By numerical simulations and theoretical derivations the effect of the various parameters on the permeation and metabolism of a drug is illustrated, tissue thickness having the strongest effect. Upon steady state, the ratio of the residence time term (i.e. L^2 / D) of a substrate in the tissue to the metabolic half-life term ($C_{S,D}$ P / $2V_{max}$), determines the concentration gradient within the tissue and the extent of metabolism. For validation of the model, permeation of the peptidomimetic Ala-4-methoxy-naphtylamine (Ala-MNA) across both HaCaT cell sheets and stripped human skin were compared to numerical simulations. Parameter estimates used for those calculations were validated in independent experiments. Experimental data was in good agreement with numerical predictions. Furthermore, parameter fitting also revealed values similar to the independently validated parameters indicating the principal validity of the model. It was shown that aminopeptidase activity is sufficiently high to completely degrade permeating Ala-MNA within the first ~25 μm of the viable epidermis of human skin.

Introduction

Transdermal drug delivery is perhaps one of the most successful controlled release technologies available today (Guy, 1996). Nevertheless, to efficiently overcome the barrier function of the skin often remains a problem. Besides the stratum corneum, representing a major physical barrier, the skin behaves also as an efficient metabolic barrier capable of degrading a wide variety of compounds (Kao and Carver, 1990; Steinsträsser and Merkle, 1995). Therefore, first-pass-type cutaneous metabolism can be a significant source of presystemic clearance of xenobiotics. For example, in rhesus monkeys cutaneous metabolism accounts for a ~20% loss in systemic bioavailability of transdermally administered nitroglycerin (Wester *et al*, 1983), and leads to a complete cutaneous cleavage of buprenorphine prodrugs (Stinchcomb *et al*, 1996).

Physical modeling is a tool to understand the kinetics of metabolic processes in living tissue and to evaluate factors effecting metabolism and related mass transport. Because diffusion and metabolism in viable tissues are mechanistically connected (Potts *et al*, 1989; Steinsträsser *et al*, 1995), the flux of intact substrate permeating a metabolizing tissue will be influenced by both mass transport and metabolism parameters. Physical models have been described in the literature to explain the interplay between mass transport and concurrent metabolism and to analyze the experimental data. Usually they are based on Fickian diffusion in combination with first order metabolic reactions (e.g. Yu *et al*, 1979a, Tojo *et al*, 1985, Sato and Mine, 1996). While the assumption of first order metabolism kinetics may hold for low drug concentrations (Higuchi *et al*, 1983), non-linear saturation kinetics is more typical for

high drug concentrations or low enzyme contents in the skin (Schäfer and Redelmeier, 1996; Sugibayashi *et al*, 1996). In those cases, saturable Michaelis-Menten kinetics, in combination with Fickian diffusion, is more appropriate to describe cutaneous metabolism.

Previously, we proposed a physical model for the quantitative interpretation of steady state mass transport and concurrent metabolism in metabolically active cell sheets under *reflection kinetics*, i.e. with an impermeable wall on one side of the tissue resulting in reflection of both substrate and metabolite fluxes (Steinsträsser et al, 1995). The model was based on Fickian diffusion in combination with saturable Michaelis-Menten kinetics to account for the metabolic cleavage. The study was run in cultured HaCaT cell sheets, a human transformed keratinocyte cell line. In a practically more relevant study we extended this work to *permeation kinetics* in cultured HaCaT cell sheets versus stripped human skin. Both data sets could be correlated on the basis of a uniform physical model (Boderke *et al*, in press). A related physical model including the stratum corneum as a second compartment was previously introduced to analyze mass transport and metabolism of ethyl nicotinate in hairless rat skin (Sugibayashi *et al*, 1996).

Here, we will illustrate the influence of various mass transport and metabolism parameters (i.e. diffusion coefficient D, tissue thickness L, partition coefficient P and maximum metabolic rate V_{max}) on the concentration gradients across metabolizing tissue. In order to validate the underlying theory we will compare numerically generated data with experimental data on the permeation of a peptidomimetic

compound through HaCaT cell culture sheets and strippend human skin. Also we present the corresponding fluxes of intact substrate which will be delivered through the tissue as a function of donor substrate concentration.

Theoretical

The physical model. Consider a layer $0 \leq x \leq L$ of metabolizing tissue of the thickness L. At the position x = 0, i.e. the donor/tissue interface, the layer is in contact with a well stirred donor solution of a defined substrate concentration $C_{S,D}$. At the position x = L, the tissue/receiver interface, the tissue is in contact with a well stirred receiver solution. Substrate partitions into the tissue according to its partition coefficient P and passes the layer by passive diffusion. Upon passage of the metabolizing tissue degradation of substrate S to metabolite M occurs. Based on the concentration gradient the generated metabolite will diffuse into both the donor and the receiver compartment. A schematic representation of the proposed model is given in Fig 1. The following assumptions were made:

- Metabolism occurs in the tissue only, and is assumed to follow Michaelis-Menten kinetics.
- For simplicity only, the distribution of the metabolically active enzymes in the layer is assumed to be homogeneous.
- Mass transport is one-dimensional and restricted to the x coordinate

Changes in the concentration of substrate C_S and metabolite C_M in the tissue as a function of time t and distance x are given by the following set of partial differential equations of parabolic type:

$$\frac{\partial C_S}{\partial t} = D_S \frac{\partial^2 C_S}{\partial x^2} - \frac{V_{max} C_S}{K_m + C_S} \qquad (1)$$

$$\frac{\partial C_M}{\partial t} = D_M \frac{\partial^2 C_M}{\partial x^2} + \frac{V_{max} C_S}{K_m + C_S} \quad (2)$$

where D_S and D_M are the effective diffusion coefficients of substrate and metabolite in the tissue, respectively, and V_{max} and K_m are the maximum metabolic rate and the Michaelis constant, respectively.

If no enzymatic activity is present, i.e. $V_{max} = 0$, only passive diffusion of the substrate occurs and the equations simplify to:

$$\frac{\partial C_S}{\partial t} = D_S \frac{\partial^2 C_S}{\partial x^2} \quad (3)$$

Under steady state conditions the changes in substrate and metabolite concentration with time are zero, therefore:

$$0 = D_S \frac{d^2 C_S}{d x^2} - \frac{V_{max} C_S}{K_m + C_S} \quad (4)$$

$$0 = D_M \frac{d^2 C_M}{d x^2} + \frac{V_{max} C_S}{K_m + C_S} \quad (5)$$

The tissue is initially considered to be free of drug and metabolite, thus the initial conditions are:

$$C_S = C_M = 0 \qquad 0 \le x \le L \text{ for } t = 0 \quad (6)$$

Assuming that drug and metabolite concentrations in the receiver as well as the metabolite concentration in the donor are zero (perfect sink conditions) boundary conditions were set as follows:

$$C_M = 0 \qquad x = 0 \tag{7a}$$

$$C_S = C_M = 0 \qquad x = L \tag{7b}$$

Substrate concentration at x = 0 is equal to the substrate concentration in the donor compartment $C_{S,D}$, corrected by the apparent tissue/buffer partition coefficient P:

$$C_S = P\, C_{S,D} \qquad x = 0 \tag{8}$$

Under *infinite dose conditions* this concentration is assumed to be constant. Alternatively we may assume a time dependent decrease of substrate concentration in the donor due to the permeation of substrate. Such *finite dose conditions* can be modeled by coupled ordinary differential equations. The amount Q of substrate S permeating from the donor through an area A into the tissue is described by:

$$Q_{S,D}(t) = -A\, D_S \int_0^t \left. \frac{d\, C_S(x,t)}{d\, x} \right|_{x=0} d\, t \tag{9}$$

The coupling to the partial differential equation is obtained by defining the new boundary condition in the form:

$$C_S\,(t) = P_S\, \frac{Q_{S,D}(t)}{V_D} \qquad x = 0 \tag{10}$$

where V_D denotes the volume of the donor solution.

Likewise the cumulative amount Q of substrate and metabolite which permeates through an area A into the donor and receiver compartment, respectively, can be obtained by the following equations:

$$Q_{S,R}(t) = -A\,D_S \int_0^t \left.\frac{d\,C_S(x,t)}{d\,x}\right|_{x=L} d\,t \tag{11}$$

$$Q_{M,D}(t) = A\,D_M \int_0^t \left.\frac{d\,C_M(x,t)}{d\,x}\right|_{x=0} d\,t \tag{12}$$

$$Q_{M,R}(t) = -A\,D_M \int_0^t \left.\frac{d\,C_M(x,t)}{d\,x}\right|_{x=L} d\,t \tag{13}$$

These cumulative amounts can be evaluated numerically and compared with experimental data. Concentration gradients of substrate and metabolite at each position x within the skin at the time t can be numerically generated from equations 1 and 2. The gradients at the interfaces will determine fluxes of substrate and metabolite:

$$J_{S,D} = D_S \left.\frac{d\,C_S}{d\,x}\right|_{x=0} \tag{14}$$

$$J_{S,R} = D_S \left.\frac{d\,C_S}{d\,x}\right|_{x=L} \tag{15}$$

$$J_{M,D} = D_M \left.\frac{d\,C_M}{d\,x}\right|_{x=0} \tag{16}$$

$$J_{M,R} = D_M \left.\frac{d\,C_M}{d\,x}\right|_{x=L} \tag{17}$$

To study the influence of the different parameters on the steady-state substrate concentration profiles within the tissue and on the resulting substrate fluxes into the receiver compartment, parameter values of L, D, V_{max} and P were separately varied in a

relevant range. For substrate and metabolite having approximately the same molecular weight their diffusion coefficients were assumed to be identical, i.e. $D = D_S = D_M$. Throughout, K_m was taken as 7 nmol ml^{-1} which is close to the experimentally obtained value for Ala-MNA in HaCaT cell homogenates. The range and the standard values applied are given in Table 1. To better compare the results of various simulations, normalized substrate and metabolite concentrations within the tissue $u = C_S(x) / C_{S,D}P$ and $v = C_M(x) / C_{S,D}P$ respectively, and normalized dimensionless distances $y = x / L$ were used.

For *non-steady state simulations* relating to experimental data a fixed set of mass transport and metabolism parameters was used. Values were taken from previously performed independent experiments (Steinsträsser, 1994; Steinsträsser *et al*, 1997): Maximum metabolic rate V_{max} and Michaelis constant K_m were derived from homogenate studies and were 9106 nmol min^{-1} ml^{-1} (corresponding to 29.7 nmol min^{-1} mg^{-1} protein) and 6.7 nmol ml^{-1}, respectively. The effective diffusion coefficients D of substrate Ala-MNA and metabolite MNA in living tissue were assumed to be $1.3 \cdot 10^{-4}$ cm^2 min^{-1} (equivalent to $\sim 2 \cdot 10^{-6}$ cm^2 s^{-1}) corresponding to data previously published by Yu *et al* (1979b) and Sugibayashi *et al* (1996). Thickness of the viable epidermis was taken as 10 µm for HaCaT cell sheets and 40 µm for stripped human skin as suggested by light micrographs. The tissue/buffer partition coefficient P of the substrate Ala-MNA, experimentally determined as octanol/buffer partition coefficient, was 0.105. To simulate the experimental conditions, finite dose conditions were considered.

Numerical Test Environment. Numerical simulation and parameter estimation results are obtained by the interactive software system EASY-FIT (Schittkowski, 1996), that allows to identify parameters in dynamic systems, especially in systems of one-dimensional, time-dependent partial differential equations with coupled ordinary differential equations. Starting from given experimental data, i.e. substrate and metabolite concentrations in donor and receiver for various observation times, the minimum least squares distance of measured values from a fitting criterion is computed, that depends on the solution of the dynamical system. For the numerical integration and parameter identification, the Fortran code PDEFIT is executed by the user interface (Schittkowski, 1997).

Basically we need to minimize

$$\sum_{k=1}^{r} \sum_{i=1}^{p} (h_k(p,t_i) - y_i^k)^2 \qquad (18)$$

where r measurement sets and p measurements per set are available. The model function $h_k(p,t)$ depends on the parameter vector p, the time variable t, but also on the solution of the underlying partial differential equation and corresponding coupled ordinary differential equations, as discussed before.

The underlying idea is to transform the set of partial differential equations into a system of ordinary differential equations by discretizing the model functions with respect to the spatial variable x. This approach is known as the method of lines (Schiesser 1991). The integration interval is divided into equidistant grid points and

first and second partial derivatives of $C_S(x,t)$ and $C_M(x,t)$ with respect to the spatial variable x are computed by a polynomial interpolation subject to the neighboring values. The number of interpolation points depends on the polynomial degree selected, i.e. the desired final accuracy. The resulting large system of ordinary differential equations is then solved by an implicit Runge-Kutta method of order 5 (Hairer and Wanner, 1991), since these equations tend to become stiff with increasing discretization accuracy.

Finally the resulting nonlinear least squares problem is solved by the code DFNLP (Schittkowski, 1988), a combination of Gauss-Newton and quasi-Newton method for constrained problems. The algorithm requires first derivatives with respect to the parameters to be estimated, which are approximated by forward differences.

Experimental

Materials. Alanine-4-methoxy-2-naphthylamide (Ala-MNA) and its metabolite 4-methoxy-2-naphthylamine (MNA) were purchased from Sigma Chemical Company (St. Louis, MO). Dulbecco's modified Eagle's medium with Glutamax®, fetal calf serum, Dulbecco's modified phosphate buffered saline with calcium and magnesium (D-PBS) and sterile glucose solution 20% (w/v) were obtained from Life Technologies, (Paisley, UK). Acetonitril was obtained from Romil Chemicals (Loughborough, UK). All other reagents were of analytical grade.

Cell Culture. HaCaT cells (donated by N. Fusenig, German Cancer Research

Institute, DKFZ, Heidelberg, Germany) were cultured on porous polycarbonate membranes (Transwell™, Costar, Cambridge, USA) for 8-9 days prior to use as previously described (Steinsträsser *et al*, 1997). The culture medium was 10 % (v/v) fetal calf serum in Dulbecco's modified Eagle's medium. Membranes were cut out with a sterile scalpel, washed three times in D-PBS and immediately used for experiments.

Preparation of the skin. Freshly excised human breast skin from cosmetic surgery was used immediately upon arrival. Fat was removed with a scalpel. Skin was stripped 20 times with adhesive tape to remove the stratum corneum, dermatomed to a thickness of ~200 μm and washed three times in fresh D-PBS to remove damaged cells.

Permeation studies. HaCaT cell culture sheets or stripped human skin were mounted between two diffusion half cells with a diffusional area of 0.64 cm^2 (Side-Bi-Side® diffusion cells, Crown Glass, Sommerville, USA), the epidermal side facing the donor chamber. The half cells were filled with 3 ml of D-PBS supplemented with 1 g l^{-1} glucose, warmed to 37°C, constantly stirred and gassed with prehumidified oxygen. To initiate the experiment, 100 μl donor solution was replaced by 100 μl of Ala-MNA stock solution to obtain initial donor substrate concentrations of 20-500 nmol ml^{-1}. Samples of 100 μl were periodically withdrawn from donor and receiver and replaced with fresh buffer. Samples were analyzed by HPLC for substrate and metabolite as previously described (Steinsträsser *et al*, 1997). All experiments were run at least in triplicate.

Numerical computations. All numerical computations including the least squares fits were performed on a PC with a Pentium® processor running under Windows®. Mass balance calculations showed less than 0.01% deviations which indicates sufficient discretization accuracy and verifies the mathematical model.

Results and Discussion

The simulated kinetic relationships of selected mass transport and metabolism parameters as obtained by numerical computation are given in Figs 2 and 3. The steady-state simulation given will focus on the effects of the diffusion coefficient D, the partition coefficient P, tissue thickness L and maximum metabolic rate V_{max}. In addition, prediction of experimental data by the theoretical model under non-steady state conditions will be demonstrated as illustrated in Figs 4 and 5. Finally, we will also cover examples of least squares fits for selected parameters.

Steady-state simulations

Diffusion coefficient D. Normalized, dimensionless substrate gradients as a function of dimensionless distance within the tissue are illustrated in Fig 2a. Various diffusion coefficients D ($D = D_S = D_M$) are considered. At high diffusivities (i.e. $D = 10^{-5}$ cm^2 s^{-1}) a nearly linear concentration gradient of substrate within the tissue is obtained. Due to the high flux of substrate permeating the tissue, metabolized substrate is efficiently replaced by fresh substrate. The fraction of metabolized drug is minor, and a practically linear concentration gradient is thus obtained. So the epidermal layer may be treated as a passive membrane as described by equation 3. On the other hand, at low diffusion coefficients (e.g. 10^{-7} or 10^{-8} cm^2 s^{-1}) the substrate concentration drops steeply with increasing distance. Consequently, due to its rate-limiting function, diffusion restricts the access of fresh substrate to the tissue. Therefore, most of the substrate will be metabolized in the upper tissue layers, with no intact substrate

reaching layers furthest from the surface. Thus, only metabolite arrives in the receiver compartment (or the systemic circulation).

Fluxes of substrate into the receiver compartment relative to the donor substrate concentration are also illustrated (Fig 2b). This depicts the potential for the substrate to reach the systemic circulation. As indicated in equations 14 and 15, influx of substrate into the tissue $J_{S,D}$ and efflux into the receiver $J_{S,R}$ will be determined by the diffusion coefficient D and the substrate concentration gradient at the donor/tissue and tissue/receiver interface, respectively. For high diffusivities the concentration gradients at y = 0 and y = 1 are practically the same. Therefore, $J_{S,R}$ and $J_{S,D}$ are almost equal and the fraction of metabolite ($F_M = 1 - J_{S,R} / J_{S,D}$) will be small. For low diffusivities (e.g. 10^{-7} or 10^{-8} cm^2s^{-1}) the concentration gradients at the tissue/receiver interface are practically zero (Fig 2a), all of the substrate will be metabolized in the top layers of the tissue and no measurable flux of substrate into the receiver occurs (Fig 2b).

Since the diffusion coefficient is related to the molecular volume of a molecule (Kasting *et al*, 1987), labile substrates of high molecular weight with a correspondingly low diffusion coefficient may have little chance to pass the metabolizing tissue under passive diffusion.

Partition coefficient P. Fig 2c presents substrate concentration gradients within the tissue for various values of the apparent tissue/donor solution partition coefficient P. A partition coefficient of 10 stands for a tenfold increased substrate concentration at the position x = 0 in comparison to the donor concentration. At high drug concentrations within the tissue (i.e. for high values of P) enzymes are expected to be

saturated and only a minor fraction of permeating substrate is metabolized. Thus, with increasing values of P the concentration gradient approaches a straight line and the tissue behaves like a passive membrane. For small values of P a greater fraction of permeating substrate is metabolized and the gradients drop steeper.

Fig 2d illustrates corresponding flux versus concentration profiles based on the aforementioned calculations. For partition coefficients smaller than 0.01 the concentration gradient at the tissue/receiver interface becomes practically zero as all of the drug is metabolized on its way through the epidermis. Therefore, no flux of intact substrate into the receiver is observed. Metabolism becomes negligible for high partition coefficients, therefore substrate flux into the receiver is roughly proportional to the substrate concentration in the donor (Fig 2d). Physically, the layer can be handled as a passive membrane according to equation 3.

Due to the relationship $C_{S,D}\ P = C_S(0)$, the parameters $C_{S,D}$ and P are physically interconnected. Therefore, Figs 3a and 3b also simulate various values of the donor substrate concentration $C_{S,D}$ at a constant partition coefficient P. Hence, for efficient transdermal delivery the substrate needs to partition well into the tissue and/or be administered at high concentration. This depends on the compound itself and on the vehicle selected for transdermal delivery. Also the use of saturated or supersaturated solutions has been suggested (Davis and Hadgraft, 1991).

Maximum metabolic rate V_{max}. The parameter V_{max} combines the concentration of metabolic enzyme present and how readily it catalyzes the reaction (London and Shaw, 1983). Increases in the maximum metabolic rate result in steeper substrate

concentration gradients within the tissue (Fig 2e) and, thus, in reduced substrate flux into the receiver (Fig 2f). The effect is similar to that observed before with the diffusion coefficient.

As expected a linear relation of substrate concentration versus distance within the tissue is observed when V_{max} is zero (Fig 2e). Correspondingly, under such conditions substrate flux into the receiver is proportional to the donor concentration as described by equation 3 (Fig 2f). For medium values of V_{max} a nonlinear relationship of the flux versus substrate concentration plot is obtained. This is explained by partial saturation of the enzymatic reaction at higher substrate concentrations. At the highest value selected the flux of intact substrate into the receiver is practically zero.

Obviously, depending on the extent of metabolic activity, the flux of drug delivered to the receiver is partially or fully reduced. Thus, for drugs susceptible to enzymatic cleavage, simultaneous delivery of a suitable enzyme inhibitor, e.g. by transdermal iontophoresis, may be a means to increase drug bioavailability. As seen in the simulations before, increases in substrate concentrations will somewhat limit the relative extent of metabolism by saturation of the enzyme.

Tissue thickness L. The effect of the tissue thickness on the overall mass transport of a drug across metabolizing tissue is depicted in Fig 3. For very thin tissue sheets (i.e. 5 μm) the flux of substrate into the sheets is sufficiently high to replace metabolized by fresh substrate almost completely. Therefore, a practically linear concentration gradient results. On the contrary, in cell sheets of 100 μm thickness, a typical thickness for the viable part of the human epidermis, a steep drop of the

concentration gradient is observed. Obviously in thick tissue diffusion is not fast enough to fully replace metabolized substrate and thus becomes rate limiting. All of the substrate will be readily metabolized in the upper portion of the tissue and, as a consequence, negligible substrate flux will result through tissue exceeding 20 μm thickness even at high donor substrate concentrations (Fig 3c). Therefore, metabolically highly labile substrates are difficult to deliver transdermally by passive diffusion alone.

The corresponding dimensionless metabolite concentration profiles for the various tissue thickness are illustrated in Fig 3b. With increasing tissue thickness the peak metabolite concentration increases and shifts towards the donor side. In 100 μm thick cell sheets all of the substrate will be degraded to its metabolite within the first ~20 μm (Fig 3a). In the remainder of the tissue no more metabolite is generated and the transport of the metabolite is only subject to passive diffusion, resulting in a linear metabolite concentration gradient with increasing relative distance x/L (Fig 3b).

Prediction of experimental data

In this theoretical analysis of simultaneous mass transport and metabolism in living tissue several assumptions were made. Assuming constant diffusivity throughout the tissue was for the sake of simplicity. Parallel to the morphological differences in polarized tissue, e.g. in the viable epidermis or in HaCaT cell sheets, also differences in diffusivities may be expected. Thus, the effective tissue diffusion coefficient will be a weighed average of the diffusivities in the various regions and routes (e.g.

transcellular versus paracellular). Also the assumption of homogeneous enzyme distribution across the tissue was for the sake of simplicity only. Indeed, by confocal microscopy we recently visualized that aminopeptidase activity was more or less evenly distributed in the viable epidermis of human skin except for so called 'hot spots' with enhanced enzyme activity, which were specifically found towards the stratum corneum (Boderke *et al*, 1997). Such regional differences in enzymatic activity can be implemented in a physical model but increase the complexity of the system. For the model calculations here, we assume even distribution of aminopeptidase activity as a first approximation.

To verify the physical model with its assumptions and to test its ability to predict experimental results, permeation experiments with HaCaT cell sheets and freshly excised stripped human skin were performed. HaCaT is a spontaneously transformed human keratinocyte cell line, preserving some of the morphological and biochemical features of normal human keratinocytes (Boukamp *et al*, 1988; Ryle *et al*, 1989). Based on this background, HaCaT cell cultures may serve as a model for the viable epidermis (Boderke *et al*, in press). Permeation experiments with the peptidomimetic model drug Ala-4-methoxy-2-naphthylamide (Ala-MNA), a substrate for aminopeptidases, were performed at different initial substrate concentrations and compared to simulated data. A fixed set of independently obtained mass transport and metabolism parameters was used for these simulations as described in the theoretical section.

A typical set of permeation data for an initial Ala-MNA donor concentration of ~500 nmol ml^{-1} with HaCaT cell sheets and with stripped human skin is given in Fig 4.

The experimental and the simulated donor and receiver concentration versus time profiles for Ala-MNA and its metabolite MNA were in close approximation. Metabolism was evident by an increase of metabolite concentration in both the donor and receiver compartments. Through HaCaT cells about 15% of intact Ala-MNA permeated within 2 h. On the other hand, no intact Ala-MNA could permeate through stripped skin. In addition, Fig 4 illustrates the resulting fluxes of intact substrate Ala-MNA through HaCaT and stripped skin as a function of initial substrate concentration. While even at high donor concentrations no measurable flux was observed through stripped skin, there was an over-proportionate increase of the Ala-MNA flux through HaCaT sheets with increasing initial substrate concentration. This trend is equally reflected by the experimental as well as the simulated data. A mechanistic explanation is the saturation of the drug-metabolizing enzymes as substrate concentration increases, thus limiting the relative extent of cutaneous metabolism. Differences between simulated and experimental data are minor, and are attributed to parameter selection. For example, the partition coefficient P applied was derived from octanol/water partitioning experiments. Biological partitioning of Ala-MNA may be different, but is experimentally not accessible.

Fig 5 shows 3-D-plots of the time-dependent Ala-MNA and MNA concentrations within the viable epidermis based on non-steady-state simulations corresponding to the permeation experiment illustrated in Fig 4. For all time points Ala-MNA is completely degraded in the first ~25 μm of the tissue. Consequently, no measurable substrate flux into the receiver compartment is obtained. Significant substrate concentrations are only

found within the first ~10 μm of the tissue, indicating that this substrate could only penetrate the upper layers of the epidermis. Peak metabolite concentrations are located at a tissue depth of ~10 μm but significant metabolite concentrations can be found throughout the tissue. Such simulations may be helpful in estimating local drug levels for topical drug delivery or toxic drug or metabolite concentrations.

Parameter estimation by least squares fit

The parameter estimation algorithm PDEFIT (Schittkowski, 1997) was used for least squares fits of the permeation data set (HaCaT sheets and stripped skin) given in Fig 4. As an example Table 2 shows estimated values for P, V_{max} and K_m and their standard deviations as well as experimental values. The numerically obtained estimates based on best fits for HaCaT sheets and stripped human skin were in close agreement, indicating the metabolic similarity of the two tissues. Equally, the estimates agreed well with the independently obtained experimental values, another verification of our model. Hence, based on the framework of the physical model, least squares fits of permeation data allow meaningful estimations of basic mass transport and metabolism parameters.

Previously, good agreement of simulations and experimental data was also demonstrated for the diffusion and concurrent metabolism of Ala-MNA under reflection conditions (Steinsträsser *et al*, 1995), for the permeation of Ala-MNA through HaCaT sheets and stripped human skin (Boderke *et al*, in press) and for the simultaneous transport and metabolism of ethyl nicotinate in full thickness hairless rat

skin (Sugibayashi *et al*, 1996). This supports the validity of the physical model. However, further studies involving additional substrates of various physical and chemical properties are needed to demonstrate the general applicability of the physical model.

Physical relations between mass transport and metabolism parameters

As indicated in equation 14 and 15 the concentration gradients at the donor/tissue interface and at the tissue/receiver interface determine the fluxes of substrate into the tissue and out of the tissue, respectively. With the details of the derivations given in the Appendix, the relationship between the parameters L, D, P, K_m and V_{max} and the differences of the squares of the concentration gradients at these two interfaces is given by:

$$\left(\frac{du}{dy}\right)^2\Bigg|_{y=0} + \left(\frac{du}{dy}\right)^2\Bigg|_{y=1} = \frac{L^2 / D}{C_{S,D}P / 2V_{max}} \left(1 + \frac{K_m}{C_{S,D}P} \ln\left(\frac{\frac{K_m}{C_{S,D}P}}{\frac{K_m}{C_{S,D}P} + 1}\right)\right) \tag{19a}$$

and by introducing the coefficients 2α and β:

$$\left(\frac{du}{dy}\right)^2\Bigg|_{y=0} + \left(\frac{du}{dy}\right)^2\Bigg|_{y=1} = 2\alpha\left(1 + \beta \ln\left(\frac{\beta}{\beta + 1}\right)\right) \tag{19b}$$

If the squares of the concentration gradients at y = 0 and y = 1, $(du/dy)^2|_{y=0}$ and $(du/dy)^2|_{y=1}$, are equal, influx of substrate into the tissue will be identical to substrate efflux out of the tissue indicating that no metabolite is generated. Hence, to minimize metabolism the difference between the two gradients should be small. This will be the case for small values of either L^2 (i.e. thin tissue, Fig 3) and V_{max} (i.e. low enzymatic

activity, Figs 2e and 2f), or high values of D (i.e. highly diffusible substrates, Figs 2a and 2b) and P (i.e. high partitioning into the tissue). The dimensionless coefficient $\beta = K_m / C_{S,D} P$ represents the ratio of the Michaelis constant K_m (i.e. substrate concentration corresponding to half-maximal velocity) relative to the substrate concentration at the donor/tissue interface. With increasing values of $C_{S,D} P$ ($C_{S,D} P \rightarrow \infty$) the expression on the right hand side of equation 19 will approach zero, indicating that high drug concentrations overcome the negative impact of metabolism on permeation.

The term L^2 / D in equation 19 may be interpreted as the *residence time* of the substrate in the tissue (Ho, 1993). The longer a substrate is in contact with metabolizing enzymes, the greater the total extent of metabolism. Since the residence time term is proportional to L^2, the impact of tissue thickness is greater than that of the diffusion coefficient. In other words, with respect to the concentration gradients, a 10-fold increase in distance L is equivalent to a 100-fold decrease of D or a 100-fold increase of V_{max}, respectively.

On the other hand, the term $C_{S,D} P / 2V_{max}$ may represent the *metabolic half-life* of the substrate under zero order kinetics (i.e. at saturation), with V_{max} being the maximum metabolic rate. Therefore, the dimensionless coefficient $2\alpha = \frac{L^2 / D}{C_{S,D} P / 2 V_{max}}$ is the ratio of the residence time term and the metabolic half-life term, and represents a relative quantity to describe the extent of metabolism. If the residence time term is small relative to the metabolic half-life term, small values for

the coefficient 2α will result, and the chance for intact substrate molecules to permeate the tissue is high. On the contrary, when a large residence time term outweighs the metabolic half-life term, 2α is high and permeation of intact substrate is blocked by efficient metabolism.

L is a key parameter for the kinetics of mass transport and concurrent metabolism as it has a quadratic impact on 2α. Whereas diffusion through thin layers (e.g. HaCaT cell culture sheets) may be fast enough to substitute metabolized substrate, permeation through thick layers (e.g. viable epidermis) may be limited by diffusion and lead to practically complete metabolization of the drug. For example, for the permeation of Ala-MNA through HaCaT cell sheets, using the fixed set of parameter values corresponding to Fig 4, 2α equals ~2.7. In contrast, as a result of a much higher residence time term for the 4-fold thicker human epidermis, 2α becomes ~43. The impact of 2α on the fraction of intact substrate reaching the receiver, $F_S = J_{S,R} / J_{S,D}$ (i.e. the ratio of substrate efflux into the receiver $J_{S,R}$ to substrate influx into the tissue $J_{S,D}$), is illustrated in Fig 6. With increasing 2α the extent of metabolism increases drastically. For $2\alpha > 10$ the fraction of intact substrate flux into the receiver becomes negligible (< 5%). Indeed, in our studies the model substrate Ala-MNA was completely metabolized in stripped human skin (2α = ~43) whereas ~40% could permeate the much thinner HaCaT sheets (2α = ~2.7; Figs 4 and 6).

The results illustrate the efficient barrier function of the skin for metabolically labile drugs. For buccal drug delivery the metabolizing tissue is even thicker (~300-

500 μm), lowering the chance for intact substrate permeating through buccal tissue, assuming, that all the other parameters are similar. In fact, as shown by Garren *et al* (1989) for the in vitro permeation of Leu-p-nitroanilide across excised buccal hamster cheek pouch epithelium, complete metabolization of the substrate was observed. Vice versa, the ability of a tissue to metabolize xenobiotics represents an important feature for prodrug approaches and for dermal toxicity considerations. Therefore, the proposed model may be also helpful for the development of prodrugs and to evaluate the toxicity of skin pollutants.

In conclusion, our studies demonstrate a quantitative framework to model diffusion and cutaneous metabolism for dermal and transdermal delivery. Mass transport and metabolism kinetics are intimately connected and determine the impact of epidermal residence and metabolic cleavage. Each of the basic parameters, i.e. tissue thickness L, diffusion coefficient D, substrate partition coefficient P, maximum metabolic rate V_{max}, and the substrate concentration in the donor $C_{S,D}$, will affect the concentration profile of the substrate within a tissue and its flux through the tissue. The coefficient 2α, i.e. the ratio of the substrate's residence time term to its metabolic half-life term, is the key determinant for the extent of metabolism during absorption. So, the considerations presented may help to develop strategies to overcome the metabolic barrier of the skin. Moreover, therapeutic or toxic substrate and metabolite levels in tissues may be calculated and the potential of a substrate to pass a metabolic barrier may be predicted. Since metabolism is a general feature of viable tissue, this model may be useful for the estimation of permeation and concurrent metabolism in other

tissues and for other substrates as well.

Acknowledgment

We thank G. Imanidis for fruitful discussions and for his critical review of the manuscript.

References

Boderke P, Bodde HE, Ponec M, Wolf M, Merkle HP: Mechanistic and quantitative prediction of aminopeptidase activity in stripped human skin based on the HaCaT cell sheet model. *J. Invest. Dermatol.* , in press

Boderke P, Merkle HP, Cullander C, Ponec M, Bodde HE: Localization Of Aminopeptidase Activity In Freshly Excised Human Skin - Direct Visualization By Confocal Laser Scanning Microscopy. *J. Invest. Dermatol.* 108:83-86, 1997

Boukamp P, Petrussevska RT, Breitkreutz D, Hornung J, Markham A, Fusenig NE: Normal keratinization in a spontaneously immortalized aneuploid human keratinocyte cell line. *J. Cell Biol.* 106:761-71, 1988

Davis AF, Hadgraft J: The use of supersaturation in topical drug delivery. In: Scott RC, Guy RH, Hadgraft J, Boddé HE (eds.). *Prediction of percutaneous penetration: Methods, Measurements, Modelling. Vol 2.* Information Press IBC Technical Services, Oxford, 1991, pp 279-287

Garren KW, Topp EM, Repta AJ: Buccal absorption . III. Simultaneous diffusion and metabolism of an aminopeptidase substrate in the hamster cheek pouch. *Pharm. Res.* 6:966-970, 1989

Guy RH: Current status and future prospects of transdermal drug delivery. *Pharm. Res.* 13:1765-9, 1996

Hairer E, Wanner G: *Solving Ordinary Differential Equations II. Stiff and Differential-Algebraic Problems,* Series Computational Mathematics, Springer, 1991

Higuchi WI, Gordon NA, Fox JL, Ho FH: Transdermal delivery of prodrugs. *Drug Development & Industrial Pharmacy* 9:691-706, 1983

Ho NFH: Biophysical kinetic modeling of buccal absorption. *Advanced Drug Delivery Reviews* 12:61-97, 1993

Kao J, Carver MP: Cutaneous metabolism of xenobiotics. *Drug Metab. Rev.* 22:363-

410, 1990

Kasting GB, Smith RL, Cooper ER: Effect of lipid solubility and molecular size on percutaneous absorption. In: Schroot B, Schäfer H (eds.). *Skin Pharmacokinetics.* Karger, Basel, 1987, pp 138-153

London JW, Shaw LM: Reaction kinetics. In: Bergmeyer HU (ed.). *Methods of enzymatic analysis. Vol 1.* Verlag Chemie GmbH, Weinheim, 1983, pp 68-85

Potts RO, McNeill SC, Desbonnet CR, Wakshull E: Transdermal drug transport and metabolism. II. The role of competing kinetic events. *Pharm. Res.* 6:119-24, 1989

Ryle CM, Breitkreutz D, Stark HJ, Leigh IM, Steinert PM, Roop D, Fusenig NE: Density-dependent modulation of synthesis of keratins 1 and 10 in the human keratinocyte line HACAT and in ras-transfected tumorigenic clones. *Differentiation* 40:42-54, 1989

Sato K, Mine T: Analysis of in vitro rat skin permeation and metabolism of SM-10902, prodrug of synthetic prostacyclin analogue. *Int. J. Pharm.* 135:127-136, 1996

Schäfer H, Redelmeier TE: *Skin Barrier: Principles of percutaneous absorption.* Karger, Basel, pp 153-212, 1996

Schittkowski K: Solving nonlinear least squares problems by a general purpose SQP-method, in: *Trends in Mathematical Optimization*, K.-H. Hoffmann, J.-B. Hiriart-Urruty, C. Lemarechal, J. Zowe eds., International Series of Numerical Mathematics, Vol. 84, Birkhäuser, 1988

Schittkowski K: Parameter estimation in one-dimensional, time-dependent partial differential equations, *Optimization Methods and Software*, Vol. 7, No. 3-4, 165-210, 1997

Schittkowski K: *EASY-FIT Version 2.0: Parameter estimation in dynamic systems - User's guide -,* Report, Department of Mathematics, University of Bayreuth, 1996

Schiesser WE: *The numerical method of lines.* Academic Press, San Diego, 1991

Steinsträsser I: The Organized HaCaT Cell Culture Sheet: A Model Approach to Study Epidermal Peptide Drug Metabolism, Pharmaceutical Technology. Zürich, Swiss Federal Institute of Technology Zürich, 1994, pp 140

Steinsträsser I, Koopmann K, Merkle HP: Epidermal aminopeptidase activity and metabolism as observed in an organized HaCaT cell sheet model. *J. Pharm. Sci.* 86:378-383, 1997

Steinsträsser I, Merkle HP: Dermal metabolism of topically applied drugs: pathways and models reconsidered. *Pharm. Acta Helv.* 70:3-24, 1995

Steinsträsser I, Sperb R, Merkle HP: Physical model relating diffusional transport and concurrent metabolism of peptides in metabolically active cell sheets. *J. Pharm. Sci.* 84:1332-41, 1995

Stinchcomb AL, Paliwal A, Dua R, Imoto H, Woodard RW, Flynn GL: Permeation of buprenorphine and its 3-alkyl-ester prodrugs through human skin. *Pharm. Res.* 13:1519-23, 1996

Sugibayashi K, Hayashi T, Hatanaka T, Ogihara M, Morimoto Y: Analysis Of Simultaneous Transport and Metabolism Of Ethyl Nicotinate In Hairless Rat Skin. *Pharm. Res.* 13:855-860, 1996

Tojo K, Valia KH, Chotani G, Chien YW: Long-term permeation kinetics of estradiol: (IV) A theoretical approach to the simultaneous skin permeation and bioconversion of estradiol esters. *Drug Dev. Ind. Pharm.* 11:1175-1193, 1985

Wester RC, Noonan PK, Smeach S, Kosobud L: Pharmacokinetics and bioavailability of intravenous and topical nitroglycerin in the rhesus monkey: estimate of percutaneous first-pass metabolism. *J. Pharm. Sci.* 72:745-8, 1983

Yu CD, Fox JL, Ho NFH, Higuchi WI: Physical model evaluation of topical prodrug delivery - simultaneous transport and bioconversion of vidarabin-5'-valerate I: Physical model development. *J. Pharm. Sci.* 68:1341-1346, 1979a

Yu CD, Fox JL, Ho NF, Higuchi WI: Physical model evaluation of topical prodrug

delivery-simultaneous transport and bioconversion of vidarabine-5'-valerate II: Parameter determinations. *J. Pharm. Sci.* 68:1347-57, 1979b

Fig 1. Schematic diagram of the physical model. C = concentration. Subscripts S and M represent substrate and metabolite, and subscripts D and R donor and receiver compartments, respectively. L denotes tissue thickness.

Fig 2. Influence of D, P and V_{max}. Simulated dimensionless concentration gradients within the tissue for (a) effective substrate and metabolite diffusion coefficients D of 10^{-8}, 10^{-7}, 10^{-6} and 10^{-5} cm^2 s^{-1}, (c) substrate partition coefficients of 0.01, 0.1, 1 and 10 and (e) various values of the maximum metabolic rates V_{max} of 0, 2, 4, 8, 16 and 80 μmol min^{-1} ml^{-1}. The corresponding resulting fluxes of substrate into the receiver compartment as a function of the donor substrate concentration are given in b, d and f respectively. Standard parameter estimates were used for all simulations as indicated in Table 1.

Fig 3. Influence of tissue thickness L. Simulated dimensionless concentration gradients for (a) substrate and (b) metabolite within 5, 10, 20 and 100 μm thick metabolizing tissue, and (c) the resulting substrate fluxes into the receiver as a function of the donor substrate concentration. Standard parameter estimates were used for both simulations as indicated in Table 1.

Fig 4. Prediction of experimental data. Typical concentration-time profiles of substrate Ala-MNA (dots) and metabolite MNA (squares) in donor and receiver compartment as

obtained in a typical permeation experiment with stripped human skin and HaCaT cell sheets (mean ± SD) at an initial Ala-MNA donor concentration of ~500 nmol ml^{-1}. Lines represent numerically generated simulations for Ala-MNA (solid line) and MNA (broken line). The corresFlux versus initial substrate concentration profile (solid line) and experimental data (mean ± SD) obtained in permeation studies with different initial Ala-MNA concentrations. Parameter values used for both simulations were: D = 2.1 10^{-6} cm^2 s^{-1}, P = 0.105, V_{max} = 9106 nmol min^{-1} ml^{-1}, K_m = 6.7 nmol ml^{-1} and thickness of viable epidermis L= 10 μm for HaCaT sheets and 40 μm for stripped human skin as determined in independent experiments (see methods). bis hier nicht korrigiert

Fig 5. Numerically generated non-steady-state concentration-time profiles of substrate Ala-MNA and metabolite MNA for viable epidermis of stripped human skin. Profiles correspond to data of Fig 4. Parameter values used for both simulations were: D = 2.1 10^{-6} cm^2 s^{-1}, P = 0.105, V_{max} = 9106 nmol min^{-1} ml^{-1}, K_m = 6.7 nmol ml^{-1} and thickness of viable epidermis L= 10 μm for HaCaT sheets and 40 μm for stripped human skin as determined in independent experiments (see methods).

Fig 6. Influence of the coefficient 2α on the extent of metabolism during permeation. The ratio F_S of efflux of intact Ala-MNA into the receiver ($J_{S,R}$) to influx of substrate into the tissue ($J_{S;D}$) was numerically generated for various values of 2α. A constant

value of 0.14, corresponding to K_m = 7 nmol ml^{-1}, P = 0.1 and C_S = 500 nmol ml^{-1}, was used for the coefficient β.

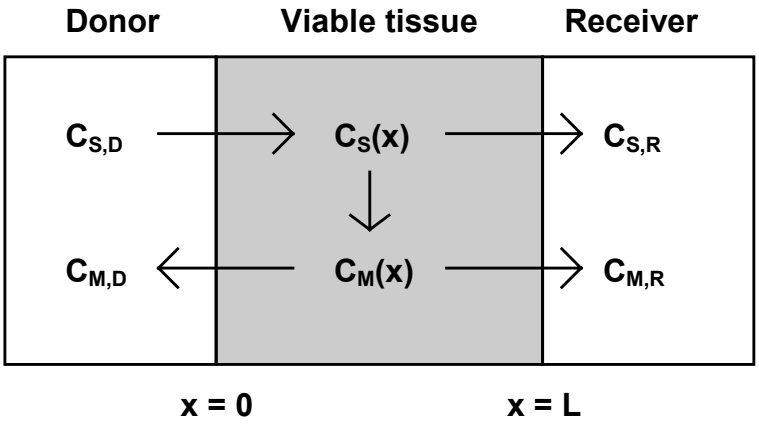

Figure 1

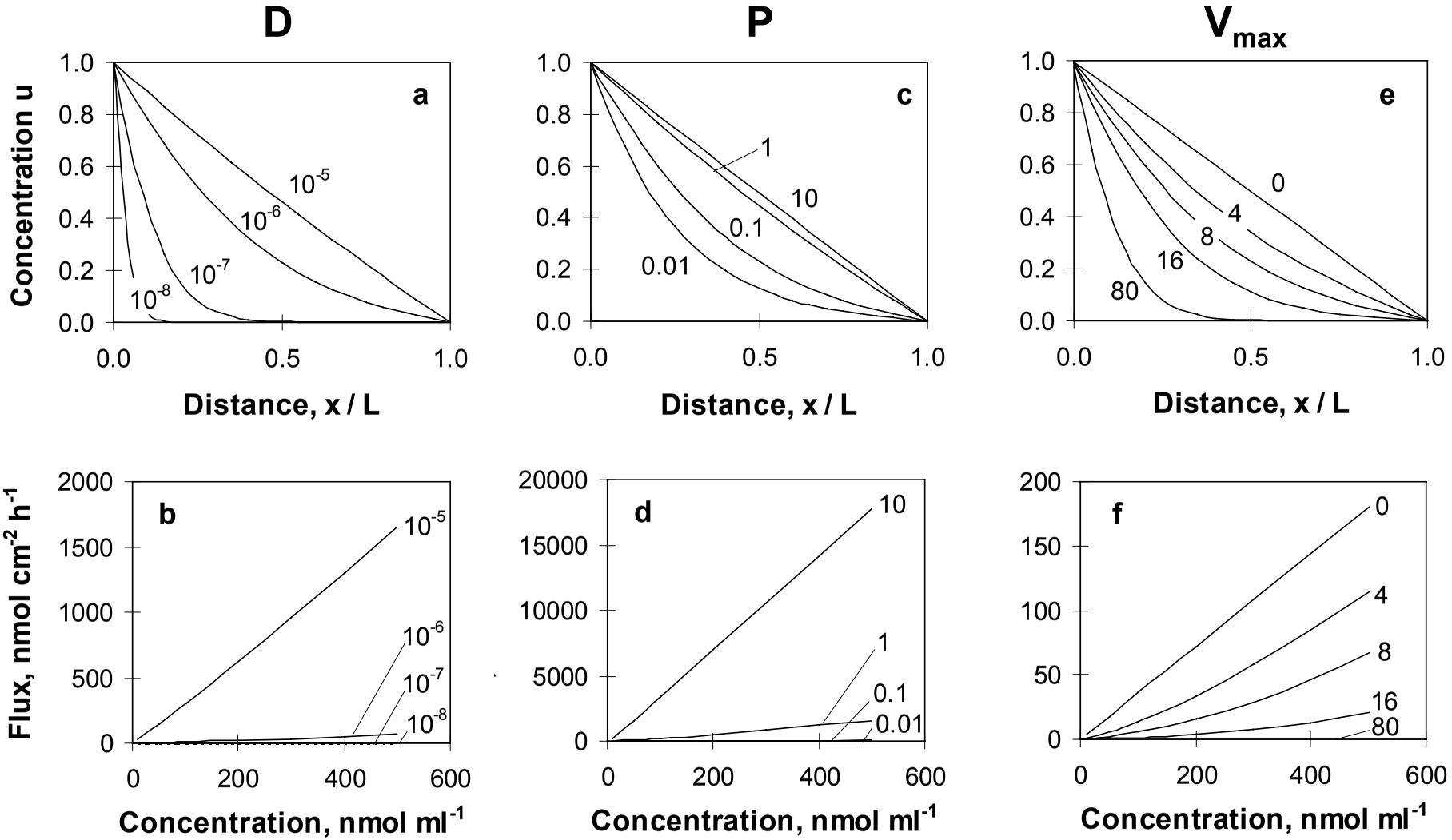
D
P
V_{max}
a
c
e
b
d
f
Concentration u
Distance, x / L
Flux, nmol cm^{-2} h^{-1}
Concentration, nmol ml^{-1}
10^{-5}
10^{-6}
10^{-7}
10^{-8}
1
10
0.1
0.01
0
4
8
16
80

Figure 2

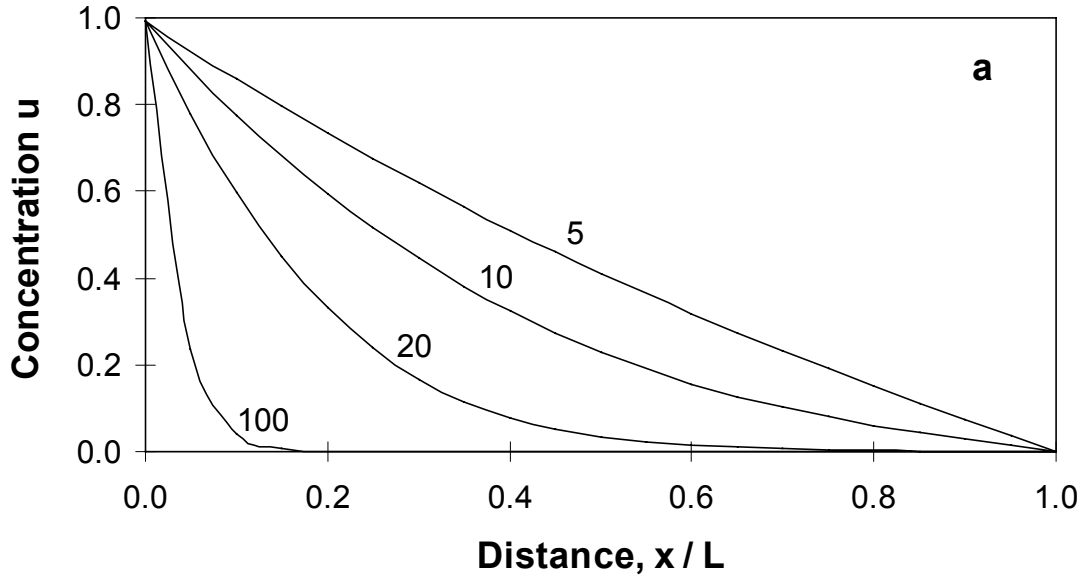
a
Concentration u
Distance, x / L
5
10
20
100
0.0
0.2
0.4
0.6
0.8
1.0

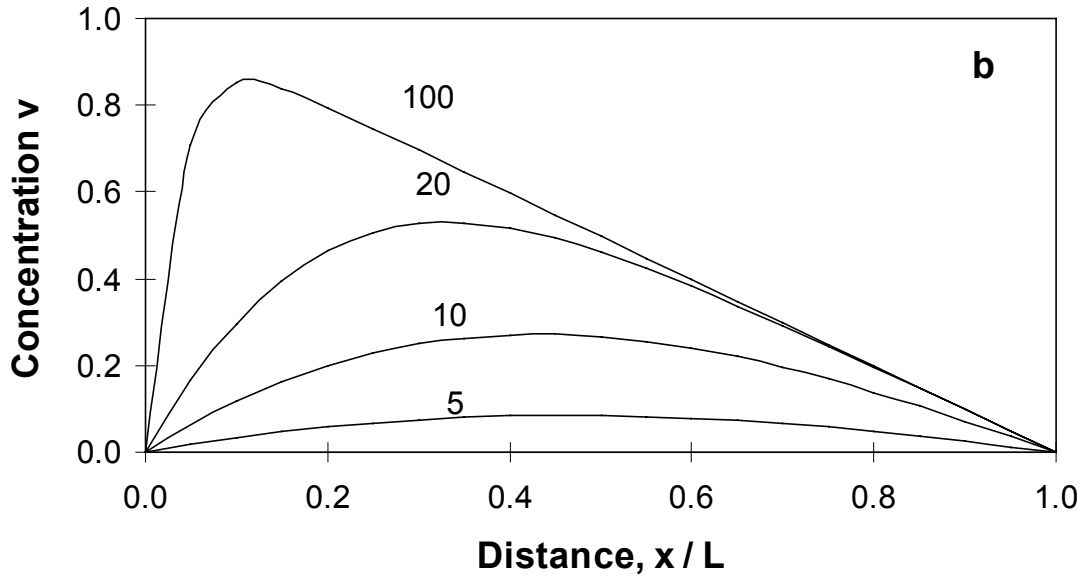
b
Concentration v
Distance, x / L
100
20
10
5
0.0
0.2
0.4
0.6
0.8
1.0

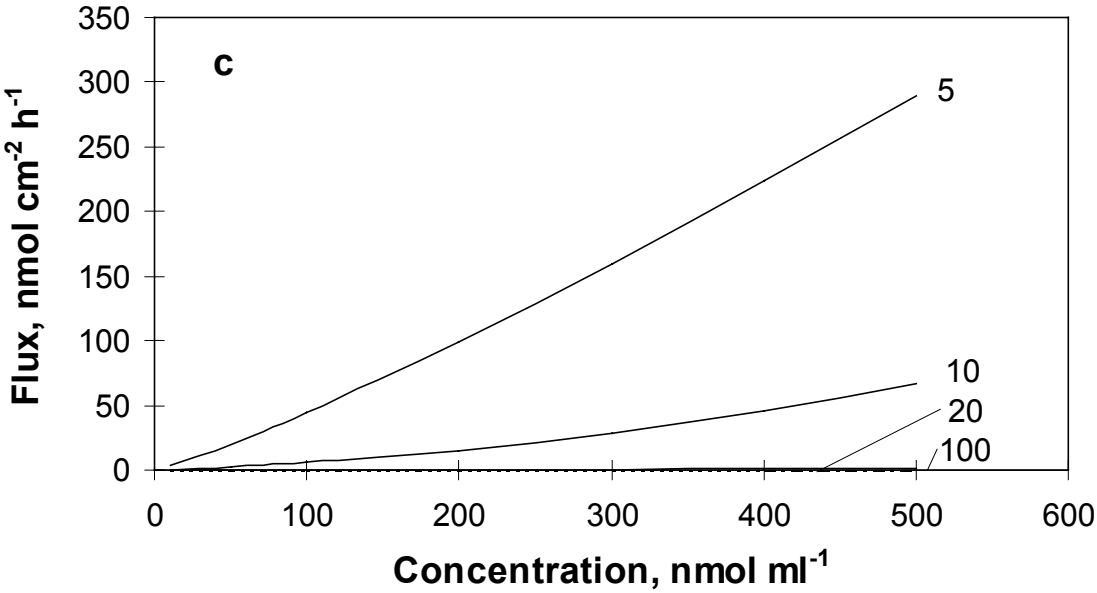
c
Flux, nmol cm-2 h-1
Concentration, nmol ml-1
5
10
20
100
0
50
100
150
200
250
300
350
0
100
200
300
400
500
600

Figure 3

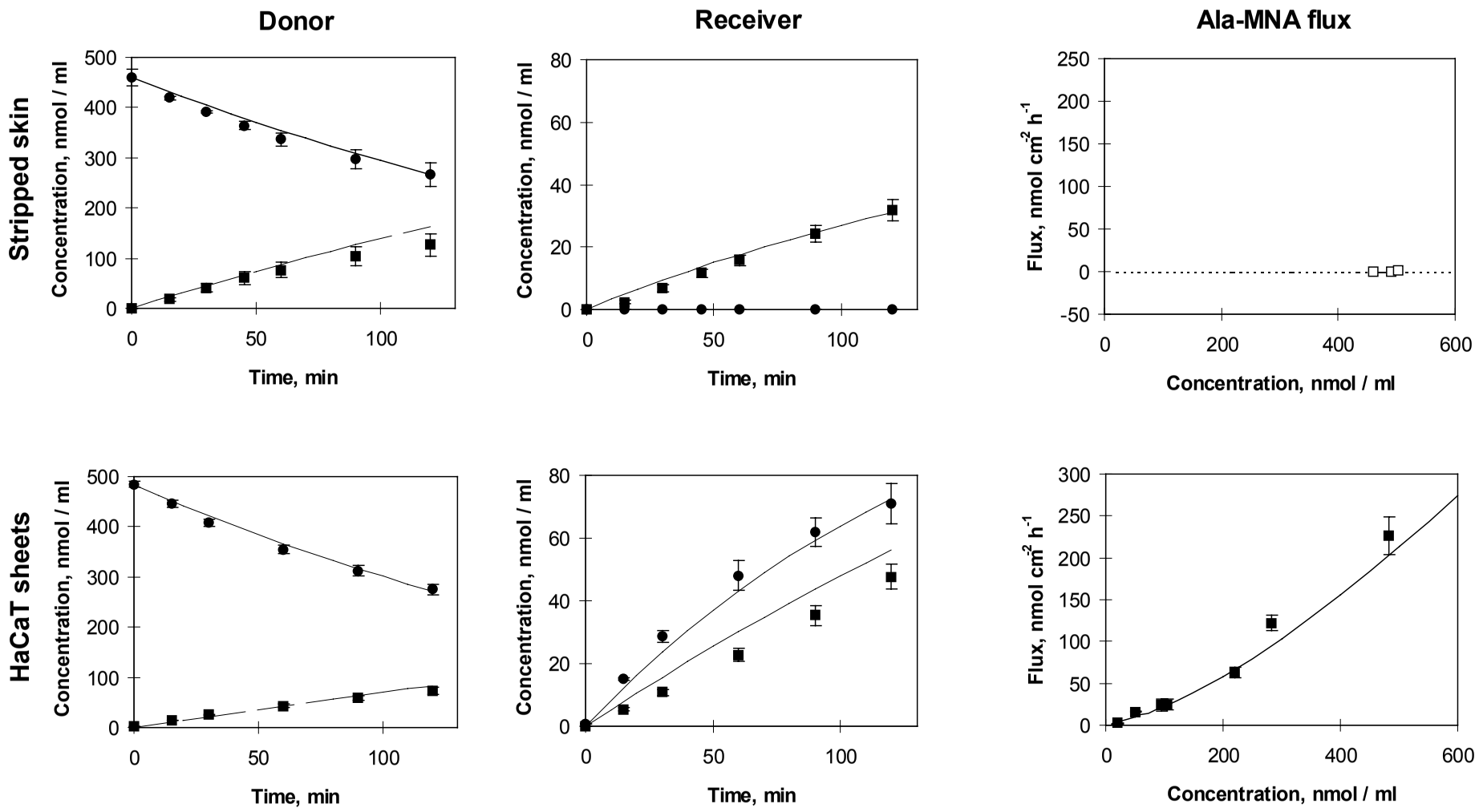
Donor
Receiver
Ala-MNA flux
Stripped skin
HaCaT sheets
Concentration, nmol / ml
Time, min
Flux, nmol cm-2 h-1
Concentration, nmol / ml

Figure 4

Figure 5

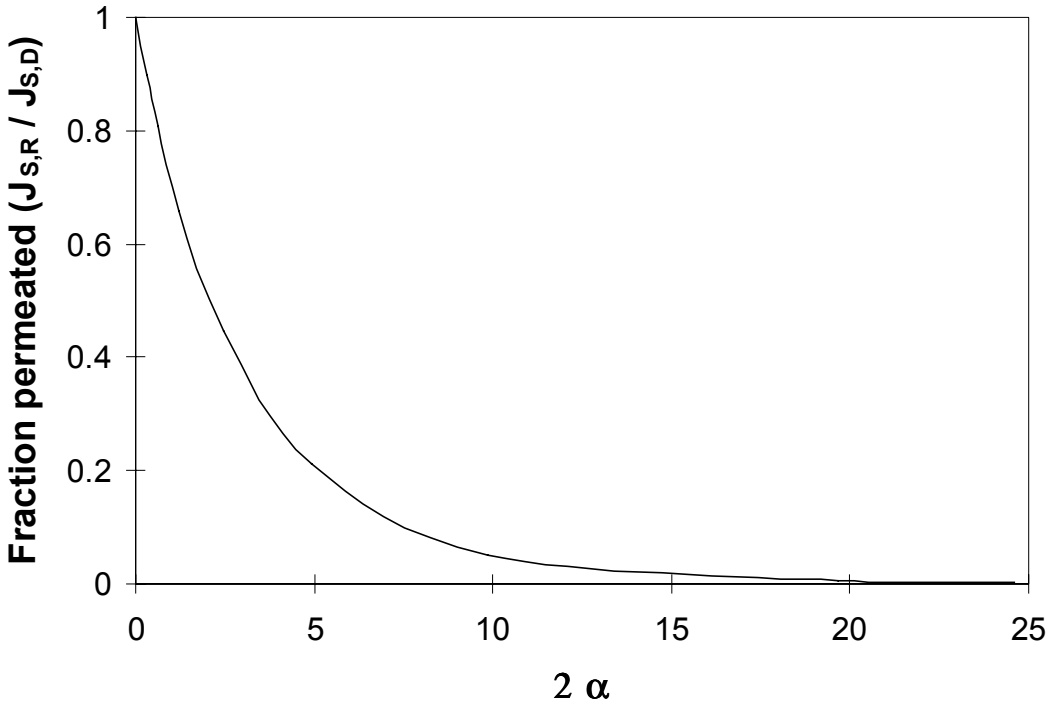

Figure 6

Table 1. Range of parameter values used for theoretical simulations[a].

L, μm	D, $cm^2\ s^{-1}$	V_{max}, nmol min^{-1} ml^{-1}	P
5	10^{-5}	4000	0.01
10	**10^{-6}**	**8000**	**0.1**
20	10^{-7}	16000	1.0
100	10^{-8}	80000	10.0

[a]Standard values in bold. A substrate concentration of $C_{S,D}$ = 300 nmol ml^{-1} and a Michaelis constant of K_m = 7 nmol ml^{-1} was chosen for all steady-state simulations.

Table 2. Numerically obtained parameter estimates ± SD from fits of the permeation experiment illustrated in Fig 4 with HaCaT sheets and stripped human skin[a].

Parameter	HaCaT sheets	Stripped skin	Experimental data
P	0.096 ± 0.002	0.101 ± 0.008	0.105 ± 0.002
V_{max} (nmol ml^{-1} min^{-1})	9200 ± 880	7580 ± 2040	9106 ± 480
K_m (nmol ml^{-1})	9.7 ± 2.1	10.1 ± 3.5	6.7 ± 2.2

[a]Fixed parameter values used for the calculations: thickness of viable epidermis L = 10 µm for HaCaT sheets and L = 40 µm for stripped skin, diffusion coefficient $D_S = D_M$ = 0,013 mm^2 min^{-1} (~$2{,}1 \cdot 10^{-6}$ cm^2 s^{-1}). SD based on standard error of regression analysis.

Appendix

Under steady state conditions the changes in substrate and metabolite concentration as a function of distance x within the metabolizing tissue are determined by the following nonlinear differential equations:

$$0 = D_S \frac{d^2 C_S}{d\,x^2} - \frac{V_{max}\, C_S}{K_m + C_S} \qquad \text{(A-1)}$$

$$0 = D_M \frac{d^2 C_M}{d\,x^2} + \frac{V_{max}\, C_S}{K_m + C_S} \qquad \text{(A-2)}$$

where D_S and D_M are the diffusion coefficients of substrate S and metabolite M in the tissue, respectively, C_S and C_M are the concentration of substrate and metabolite at the positon x within the tissue, V_{max} is the maximum metabolic rate and K_m is the Michaelis constant.

The boundary conditions are:

$C_S = P\, C_{S,D}$ $\qquad$ (x = 0) $\qquad$ (A-3)

$C_M = 0$ $\qquad$ (x = 0) $\qquad$ (A-4)

$C_S = C_M = 0$ $\qquad$ (x = L) $\qquad$ (A-5)

where $C_{S,D}$ is the substrate concentration in the donor solution and P is the apparent tissue/donor partition coefficient. Position x = 0 corresponds to the donor/tissue interface and position x = L corresponds to the tissue/receiver interface (see Fig 1).

Adding the two differential equations A-1 and A-2 results in:

$$0 = D_S \frac{d^2 C_S}{d x^2} + D_M \frac{d^2 C_M}{d x^2} \qquad \text{(A-6)}$$

A first integral of equation A-6 is:

$$a = D_S \frac{d C_S}{d x} + D_M \frac{d C_M}{d x} \qquad \text{(A-7)}$$

Further integration leads to equation A-8:

$$D_S C_S(x) + D_M C_M(x) = a x + b \qquad \text{(A-8)}$$

where a and b are constants.

From the boundary conditions at x = 0 (equations A-3 and A-4) we conclude that:

$$b = D_S P C_{S,D}, \qquad \text{(A-9)}$$

and from the boundary condition at x = L (equation A-5) we can conclude that

$$0 = a L + D_S P C_{S,D} \qquad \text{(A-10)}$$

$$a = - D_S P C_{S,D} / L \qquad \text{(A-11)}$$

With $D_S = D_M = D$ one finds:

$$D C_S (x) + D C_M (x) = D P C_{S,D} (1 - x/L) \qquad \text{(A-12)}$$

$$C_S(x) + C_M (x) = P C_{S,D} (1-x/L) \qquad \text{(A-13)}$$

Equation A-13 shows, that for each position x within the tissue the sum of the concentrations of substrate and metabolite is equal to the linear concentration drop of the substrate throughout the tissue as observed under passive diffusion.

For dimensionless equations we introduce:

$$u(x) = \frac{C_S(x)}{C_{S,D}\,P} \tag{A-14}$$

$$y = \frac{x}{L} \tag{A-15}$$

Inserting A-14 and A-15 into A-1 and assuming, that $D_S = D_M = D$ results in:

$$D\frac{1}{L^2}C_{S,D}\,P\frac{d^2u}{dy^2} = \frac{V_{max}\,C_{S,D}\,P\,u}{K_m + C_{S,D}\,P\,u} \tag{A-16}$$

or

$$\frac{d^2u}{dy^2} = \frac{L^2}{D}V_{max}\,\frac{u}{K_m + C_{S,D}P\,u} = \frac{L^2\,V_{max}}{D\,C_{S,D}\,P}\,\frac{u}{\frac{K_m}{C_{S,D}\,P} + u} \tag{A-17}$$

We define the dimensionless quantities α and β as follows:

$$\alpha = \frac{L^2 V_{max}}{D C_{S,D} P} \tag{A-18}$$

$$\beta = \frac{K_m}{C_{S,D} P} \tag{A-19}$$

equation A-17 then becomes:

$$\frac{d^2u}{dy^2} = \alpha\frac{u}{\beta + u} \qquad 0 < y < 1 \tag{A-20}$$

with the boundary conditions:

$$u\,(0) = 1 \qquad \text{(donor side)} \tag{A-21}$$

$u(1) = 0$ (receiver side) (A-22)

We define:

$$f(u) = \frac{u}{\beta + u} \tag{A-23}$$

multiplicating equation A-20 by du/dy and inserting f(u) leads to:

$$\frac{d^2u}{dy^2}\frac{du}{dy} = \alpha f(u)\frac{du}{dy} \tag{A-24}$$

Using the expressions of equation A-25 and A-26:

$$\frac{d^2u}{dy^2}\frac{du}{dy} = \frac{1}{2}\frac{d}{dy}\left(\frac{du}{dy}\right)^2 \tag{A-25}$$

$$f(u)\frac{du}{dy} = \frac{d}{dy}\left(F(u)\right) \tag{A-26}$$

where F(u) is the antiderivative of f(u), we can write equation A-24 as follows:

$$\frac{1}{2}\frac{d}{dy}\left(\frac{du}{dy}\right)^2 = \alpha\frac{d}{dy}F(u) \tag{A-27}$$

$$\frac{d}{dy}\left[\frac{1}{2}\left(\frac{du}{dy}\right)^2 - \alpha F(u)\right] = 0 \tag{A-28}$$

By integration we get equation A-29:

$$\frac{1}{2}\left(\frac{du}{dy}\right)^2 - \alpha F(u) = \text{constant} \tag{A-29}$$

Applying the boundary condition at y = 0 (A-21) and at y = 1 (A-22) we get:

$$\frac{1}{2}\left(\frac{du}{dy}\right)^2 - \alpha F(u)\Big|_{y=0} = \frac{1}{2}\left(\frac{du}{dy}\right)^2 - \alpha F(u)\Big|_{y=1} \tag{A-30}$$

$$\frac{1}{2}\left(\frac{du}{dy}\right)^2\Big|_{y=0} - \frac{1}{2}\left(\frac{du}{dy}\right)^2\Big|_{y=1} = \alpha F(u(0)) - \alpha F(u(1)) \tag{A-31}$$

With rearrangement of equation A-23:

$$f(u) = \frac{u}{\beta + u} = \frac{\beta + u}{\beta + u} - \frac{\beta}{\beta + u} = 1 - \frac{\beta}{\beta + u} \tag{A-32}$$

one gets:

$$F(u) = u - \beta \ln(\beta + u) \tag{A-33}$$

and therefore A-31 becomes:

$$\left(\frac{du}{dy}\right)^2\Big|_{y=0} - \left(\frac{du}{dy}\right)^2\Big|_{y=1} = 2\alpha\left(1 - \beta \ln(\beta + 1) + \beta \ln(\beta)\right) \tag{A-34}$$

or

$$\left(\frac{du}{dy}\right)^2\Big|_{y=0} - \left(\frac{du}{dy}\right)^2\Big|_{y=1} = 2\alpha\left(1 + \beta \ln\left(\frac{\beta}{\beta + 1}\right)\right) \tag{A-35}$$